



HAL
open science

Metabolomics and lipidomics to identify biomarkers of effect related to exposure to non-dioxin-like polychlorinated biphenyls in pigs

Maykel Hernández-Mesa, Luca Narduzzi, Sadia Ouzia, Nicolas Soetart, Laetitia Jaillardon, Yann Guitton, Bruno Le Bizec, Gaud Dervilly

► To cite this version:

Maykel Hernández-Mesa, Luca Narduzzi, Sadia Ouzia, Nicolas Soetart, Laetitia Jaillardon, et al. Metabolomics and lipidomics to identify biomarkers of effect related to exposure to non-dioxin-like polychlorinated biphenyls in pigs. *Chemosphere*, 2022, 296, pp.133957. 10.1016/j.chemosphere.2022.133957 . hal-04021967

HAL Id: hal-04021967

<https://hal.inrae.fr/hal-04021967v1>

Submitted on 22 Jul 2024

HAL is a multi-disciplinary open access archive for the deposit and dissemination of scientific research documents, whether they are published or not. The documents may come from teaching and research institutions in France or abroad, or from public or private research centers.

L'archive ouverte pluridisciplinaire **HAL**, est destinée au dépôt et à la diffusion de documents scientifiques de niveau recherche, publiés ou non, émanant des établissements d'enseignement et de recherche français ou étrangers, des laboratoires publics ou privés.



Distributed under a Creative Commons Attribution - NonCommercial 4.0 International License

1 **METABOLOMICS AND LIPIDOMICS TO IDENTIFY BIOMARKERS OF EFFECT**
2 **RELATED TO EXPOSURE TO NON-DIOXIN-LIKE POLYCHLORINATED**
3 **BIPHENYLS IN PIGS**

4 Maykel Hernández-Mesa^{1*}, Luca Narduzzi¹, Sadiá Ouzia, Nicolas Soetart, Laetitia Jaillardon, Yann
5 Guitton, Bruno Le Bizec, Gaud Dervilly*

6 Oniris, INRAE, LABERCA, 44300 Nantes, France

7 ***Corresponding authors:**

8 *E-mail addresses:* laberca@oniris-nantes.fr; gaud.dervilly@oniris-nantes.fr (G. Dervilly) and
9 maykelhm@ugr.es (M. Hernández-Mesa)

10 **ABSTRACT**

11 Recent epidemiological studies show that current levels of exposure to polychlorinated biphenyls
12 (PCBs) remain of great concern, as there is still a link between such exposures and the development of
13 chronic environmental diseases. In this sense, most studies have focused on the health effects caused
14 by exposure to dioxin-like PCBs (DL-PCBs), although chemical exposure to non-dioxin-like PCB
15 (NDL-PCB) congeners is more significant. In addition, adverse effects of PCBs have been
16 documented in humans after accidental and massive exposure, but little is known about the effect of
17 chronic exposure to low-dose PCB mixtures. In this work, exposure to Aroclor 1260 (i.e. a
18 commercially available mixture of PCBs consisting primarily of NDL-PCBs congeners) in pigs is
19 investigated as new evidence in the risk assessment of NDL-PCBs. This animal model has been
20 selected due to the similarities with human metabolism and to support previous toxicological studies
21 carried out with more frequently used animal models. Dietary exposure doses in the order of few
22 ng/kg body weight (b.w.) per day were applied. As expected, exposure to Aroclor 1260 led to the
23 bioaccumulation of NDL-PCBs in perirenal fat of pigs. Metabolomics and lipidomics have been
24 applied to reveal biomarkers of effect related to Aroclor 1260 exposure, and by extension to NDL-
25 PCB exposure, for 21 days. In the metabolomics analysis, 33 metabolites have been identified (level 1
26 and 2) as significantly altered by the Aroclor 1260 administration, while in the lipidomics analysis, 39
27 metabolites were putatively annotated (level 3) and associated with NDL-PCB exposure. These
28 biomarkers are mainly related to the alteration of fatty acid metabolism, glycerophospholipids
29 metabolism and tryptophan-kynurenine pathway.

30 **Keywords:** hazard identification, metabolomics, polychlorinated biphenyls, mass spectrometry,
31 chemical risk analysis

¹ Present address: Department of Analytical Chemistry, Faculty of Sciences, University of Granada, Av. Fuentenueva s/n, E-18071 Granada, Spain

32 1. Introduction

33 The Stockholm Convention sets the goal of reducing and ultimately eliminating the production and
34 release of persistent organic pollutants (POPs), such as PCBs, into the environment due to their
35 toxicity to human health and ecotoxicity (Xu et al., 2013). PCBs comprise a chemical class of 209
36 congeners consisting of a thermodynamically stable chlorine-substituted biphenyl ring. Two classes of
37 PCBs have been classified according to their toxicological properties, dioxin-like PCBs (DL-PCBs) (n
38 = 12), which have an analogous toxicity to dioxins, and non-dioxin-like PCBs (NDL-PCBs) (EFSA,
39 2005). About 1,3 million tons of PCBs were produced between 1930 and 1993 for use in various
40 materials and applications due to their physico-chemical properties, including non-flammability,
41 chemical stability, high boiling point, and high dielectric constants (IARC, 2016). Commercial
42 production of PCBs was initially banned by the Toxic Substances Control Act (TSCA) in the United
43 States in 1979 due to their risks for human health, and this prohibition has been subsequently adopted
44 by almost all industrialized countries since the late 1980s. However, PCBs are currently present as
45 environmental pollutants even in the most remote regions of the world (Carlsson et al., 2018)(Kim et
46 al., 2021).

47 The ubiquitous presence of PCBs in the environment has made their toxic effects a public health
48 concern for a long time because these chemicals are still detected in human samples (Weitekamp et al.,
49 2021). Epidemiologic data suggest that body burdens of DL-PCBs and dioxins are at (or near) the
50 point where adverse health effects may be occurring; therefore, greater efforts are required to reduce
51 exposure to PCBs in order to prevent health (White and Birnbaum, 2009). The main sources of
52 exposure to PCBs are diet, especially fat-containing foods, and indoor air due to the extensive use of
53 PCBs in building materials (Grimm et al., 2015)(Lehmann et al., 2015). In 2005, the European Food
54 Safety Agency (EFSA) indicated that more than 90% of exposure to NDL-PCBs in the general
55 population is related to dietary exposure and estimated that the daily dietary intake of total NDL-PCBs
56 was between 10 and 45 ng/kg b.w. per day (EFSA, 2005). Depending on the context of the study or
57 investigation, specific congeners may be monitored. For instance, the Stockholm Convention on POPs
58 recommends the measurement of six indicator PCBs (PCB28, PCB52, PCB101, PCB138, PCB153,
59 and PCB180) to characterize NDL-PCB contamination. These NDL-PCBs are the most frequently
60 detected and represent 50% of the total PCB concentration. The second French Total Diet Study has
61 shown that mean exposure (95th percentile) to these six indicator PCBs is estimated at 2.7 (7.9) ng/kg
62 b.w. per day in the adult population. Recently, in the French Infant Total Diet Study, the exposure
63 levels to the six indicator PCBs were estimated between 0.87 and 3.53 ng/kg b.w. per day in children
64 between 1 and 36 months of age (Hulin et al., 2020). In the aforementioned cases, it was observed that
65 in some age groups the tolerable daily intake was exceeded. In this sense, tolerable daily intake s of 20
66 and 10 ng/kg b.w. per day have been established for total PCB exposure and exposure to the six
67 indicator PCBs, respectively (AFSSA, 2007)(Faroon et al., 2003).

68 The chemical risks of PCBs are related to their persistence, bioaccumulation, and toxicity which
69 depends on the PCB congener. Animal toxicology studies show that PCB mixtures with larger
70 percentages of congeners with higher chlorine content and DL-PCBs carry an increased risk of liver
71 toxicity and disturbance of thyroid function; however, similar results have been obtained for such
72 mixtures and for PCB mixtures with lower chlorine content in immunotoxicity and neurotoxicity
73 assays (Christensen et al., 2021). Although NDL-PCBs are present in a higher proportion in
74 environmental PCB mixtures, risk assessments of PCBs have traditionally focused on the effects of
75 DL-PCB congeners because they generally exert more potent toxic effects (Pikkarainen et al.,
76 2019)(Alarcón et al., 2021). Nevertheless, government agencies such as the EFSA and the Joint
77 FAO/WHO Expert Committee on Food Additives (JECFA) have recently pointed out the need to
78 address the possible adverse health effects associated with exposure to NDL-PCBs, especially in the
79 early life stage (EFSA, 2005)(JECFA, 2016). Recent studies suggest that NDL-PCBs are primarily
80 responsible for the developmental neurotoxicity associated with PCB exposure (Klocke and Lein,
81 2020). Although their role in occupational hepatotoxicity caused by higher exposure levels has been
82 known for a long time, NDL-PCBs as well as DL-PCB congeners have also recently been associated
83 with an environmental liver disease, specifically nonalcoholic fatty liver disease (Wahlang et al.,
84 2019). In this framework, there is a great concern about the risks associated with environmental and
85 dietary exposure to chemicals with endocrine disrupting properties such as PCBs, as they have
86 recently been identified as one of the main factors to contributing to the rapid increase in the incidence
87 of metabolic diseases such as nonalcoholic fatty liver disease (Heindel et al., 2017). In addition, it is
88 necessary to improve knowledge about the mechanisms by which these environmental exposures
89 induce toxic effects. Thus, later, they can be applied to relevant disease models to determine the
90 importance of chronic environmental exposure to low chemical doses to the initiation and/or
91 progression of disease etiologies (Armstrong and Guo, 2019).

92 ‘Omics approaches have recently emerged as interesting alternative methodologies to address the risk
93 assessment of chemicals and involve a shift in the way toxicological studies are conducted, from
94 identifying apical endpoints of toxicity to understanding the mechanisms of toxicity (EFSA, 2014). In
95 this sense, the identification of effect biomarkers by ‘omics contributes to reveal the mode of action of
96 chemicals, which encompasses a sequence of plausible biological events in the organism caused by
97 exposure to a chemical hazard and leads to an observed effect (Simon et al., 2014). Although
98 transcriptomics has been the most widely applied ‘omics approach in chemical risk assessment, the
99 implementation of proteomics and, especially, metabolomics has experienced increasing interest in the
100 last decade (Pielaat et al., 2013)(Hernández-Mesa et al., 2021). The metabolome is the biological layer
101 closest to the phenotype and the exposure environment, so up- and/or down-regulated metabolites may
102 be directly associated with the effects of chemical exposure. Investigating metabolome disturbances
103 represents a straightforward strategy to assess the biological plausibility of chemicals and establish

104 their mode of action (Wishart, 2016). In recent years, metabolomics has been explored as an efficient
105 methodology to carry out the risk assessment of a wide range of chemicals (Orešič et al., 2020)(Dai et
106 al., 2020)(Olesti et al., 2021), including environmental contaminants such as PCBs (Shi et al.,
107 2012)(Carrizo et al., 2017)(Pikkarainen et al., 2019)(Deng et al., 2019)(Zhang et al., 2020). In this
108 context, metabolomics is required to not only focus on revealing the mode of action of chemicals, but
109 also address current risk assessment challenges such as effects related to chemical co-exposures and
110 exposures at low dose levels (Hernández-Mesa et al., 2021). Many toxicological studies for risk
111 assessment of PCBs involved exposure doses that imply obvious toxicity; therefore, the results are
112 only representative in human populations after accidental and massive exposure (Ulbrich and
113 Stahlmann, 2004). Metabolomics provides the advantage of revealing early biomarkers of effect that
114 may be related to an adverse response of the body to low-dose chemical exposure scenarios, and which
115 manifest before visible toxicity. Consequently, metabolomics makes it possible to detect the presence
116 or absence of an effect even when the latter goes unnoticed by other toxicological methods (Pielaat et
117 al., 2013)(Viant et al., 2019)(Hernández-Mesa et al., 2021).

118 The objective of this study is to identify biomarkers of effect associated with PCB exposure at dietary
119 exposure levels. Previous animal toxicology studies applying metabolomics have typically evaluated
120 the effects of PCB exposure using mice as animal model (Shi et al., 2012)(Petriello et al., 2018)(Deng
121 et al., 2019)(Lim et al., 2020). Although less used for obvious reasons of infrastructure requirements
122 and associated costs, the pig is recognized as a relevant animal model for the study of endocrine
123 disruptors (Yang et al., 2020). In addition to a lifespan that allows for significant accumulation of
124 environmental pollutants, it shows phylogenetic, physiological, nutritional, and pathological
125 similarities with humans. Therefore, it is increasingly used in toxicology and biomedical research.
126 Therefore, this work proposes a combined metabolomics-lipidomics approach to investigate PCB
127 exposure in pigs as new piece of evidence for PCB risk assessment. To our knowledge, it is the first
128 time that metabolomics/lipidomics has been applied to the discovery of biomarkers of effect related to
129 PCB exposure in pig serum. In addition, an exposure dose of 20 ng/kg b.w. per day of a 'PCB
130 cocktail', consisting primarily of NDL-PCBs (Aroclor 1260 mixture), was selected as an approach to
131 investigate the effects on the metabolism caused by exposure to NDL-PCBs at dietary exposure levels
132 according to the second French Total Diet Study outcomes (Siroto et al., 2012). Aroclor 1260 was
133 selected for this study because its composition best mimics the bioaccumulation of PCBs found in
134 human adipose tissue (Wahlang et al., 2014).

135 **2. Material and methods**

136 **2.1 Materials and reagents**

137 All reagents and solvents used in this study were of analytical grade unless otherwise specified.
138 Acetonitrile (MeCN), methanol (MeOH), isopropanol (IPA), acetic acid, and ammonia were supplied

139 by Honeywell (Bucharest, Romania). Ultra-pure water was acquired from VWR (Fontenay-sous-Bois,
140 France), while chloroform was purchased from Carlo Erba Reactifs (SDS, Peypin, France).
141 Ammonium acetate salt (Emsure grade) was purchased from Merck (Darmstadt, Germany).
142 Metabolomics isotope-labeled internal standards (L-leucine-5,5,5-d₃, L-tryptophan-2,3,3-d₃, indole-
143 2,4,5,6,7-d₅-3-acetic acid, and 1,14-tetradecanedioic-d₂₄ acid) were from Sigma–Aldrich (Saint
144 Quentin Fallavier, France) and from CDN Isotopes (Québec, Canada). Lipidomics internal standards
145 [(LPC (15:0), PC (15:0/15:0), and TG (17:0/17:0/17:0)] were purchased from Avanti Polar Lipids
146 (Alabaster, Alabama, USA). MSCAL6 ProteoMass LTQ/FT-Hybrid standard mixtures used for
147 calibration of the MS instrument were obtained from Sigma–Aldrich (Saint Quentin Fallavier, France).
148 Aroclor 1260 (certified reference material, 1000 µg/mL in isooctane) was supplied by Sigma–Aldrich
149 (Saint Quentin Fallavier, France).

150 **2.2 Animal experimental design**

151 Six 4-month-old female pigs (Terrena, France) weighting 29.8 ± 2.3 kg were randomly assigned to
152 control (n = 2 animals) and exposed (n = 4 animals) groups. The animal experiment was carried out
153 for 32 days and consisted of three different stages (i.e. periods of acclimatization, exposure, and
154 detoxification), as shown in **Figure 1**. During the exposure period, exposed pigs received orally a
155 daily dose, of Aroclor 1260 (20 ng/kg b.w.) in 20 mL of sunflower oil whereas a 20 mL placebo of
156 sunflower oil was administrated orally to the control group. Aroclor 1260 is a mixture of highly
157 chlorinated PCBs (60% chlorine by weight) that contains 30.7% by weight of the six NDL-PCBs
158 known as the six indicator PCBs (i.e. PCB28, PCB52, PCB101, PCB138, PCB153 and PCB180)
159 (Rushneck et al., 2004). The exposure dose selected for this study (6.1 ng/kg b.w. per day 6 NDL-
160 PCBs) was based on the observed P95 exposure level of the French population to the six PCB
161 indicators in the second Total Diet Study (i.e. 7.9 ng/kg b.w. per day) (Sirot et al., 2012). This
162 exposure level is also close to but slightly lower than the tolerable daily intake of the 6 NDL-PCBs
163 (i.e. 10 ng/kg b.w. per day) (AFSSA, 2007)(Faroon et al., 2003).

164 Blood samples from control and exposed pigs were collected on days (D) 2, 4, 8, 11, 16, 19, 22, 26, 29
165 and 32. Animals were euthanized just after the last blood sampling point and several tissues and
166 organs, including perirenal fat, were recovered for further investigation. The blood samples were
167 allowed to clot at room temperature, recovering the serum part by centrifugation. Aliquots of serum
168 samples were subsequently stored at -80°C.

169 The animal study was approved by the French Ethical Committee (n°6) under project agreement
170 APAFIS#15159-2018051920446340 v2 (ONIRIS agreement E44271).

171 **2.3 Sample preparation**

172 The extraction of metabolites and lipids from serum samples was performed with a biphasic solvent
173 system [(1) MeOH + water and (2) chloroform] (Peng et al., 2017). Briefly, 30 μ L of serum were
174 extracted with 190 μ L of cold MeOH containing the metabolomics isotope-labeled internal standards
175 (1 μ g/mL), 390 μ L of cold chloroform containing the lipidomics isotope-labeled internal standards (1
176 μ g/mL) and 120 μ L of pure water. The samples were vigorously vortexed and centrifuged at 3500 g
177 for 20 minutes at 4 °C. For metabolomics and lipidomics analyses, 95 μ L of the upper or aqueous
178 phase (MeOH + water) and 200 μ L of the chloroform phase were collected, respectively. Pooled
179 quality control (QC) samples (i.e. a mixture of aliquots from the entire sample set) and extraction
180 blanks (water samples) were extracted and processed as the serum samples.

181 **2.4 UHPLC-HRMS analysis**

182 Metabolomics and lipidomics analyses were carried out on an Ultimate® 3000 Series HPLC system
183 coupled to a hybrid quadrupole-Orbitrap (Q-Exactive™) mass spectrometer (ThermoFisher Scientific,
184 Bremen, Germany) equipped with a heated electrospray (H-ESI II) source. The HRMS instrument was
185 set in dual polarity (positive/negative) acquisition mode. Metabolomics analyses were performed on a
186 Hypersil Gold C18 column (2.1 \times 100 mm, 1.9 μ m particle size; Thermo Fisher Scientific) coupled
187 with the corresponding guard column, whereas lipidomics analyses were performed on an Acquity®
188 CSH C18 (column (2.1 \times 100 mm, 1.7 μ m particle size; Waters, Manchester, UK) coupled with the
189 corresponding guard column. For metabolomics analyses, chromatographic conditions, ESI source
190 conditions and MS tuning parameters were the same as previously reported (Peng et al., 2017). For
191 lipidomics analyses, a previously described non-targeted UHPLC-HRMS workflow was selected
192 (Marchand et al., 2021). For either metabolomics or lipidomics analysis, samples were randomized
193 and divided into three batches for analysis. Data acquisition was carried out following the quality
194 assurance (QA) plan described in the Supplementary Material.

195 QC samples were also submitted to data-dependent acquisition (DDA) to generate fragmentation
196 spectra of the five most intense peaks per scan. For lipidomics, DDA experiments were replicated 3
197 times for each polarity, providing an exclusion list of peaks already fragmented in the previous
198 analysis, to obtain fragmentation data of more chromatographic peaks. For metabolomics, selected
199 reaction monitoring mode was also applied to target the features highlighted by the statistical analysis
200 as potential biomarkers.

201 **2.5 Data preprocessing**

202 LC-HRMS raw data files were initially preprocessed with Xcalibur 2.2 to check the analytical
203 performance of the method, evaluating retention time and signal intensity of internal standards. The
204 raw (*.raw) files were converted to *.mzML format and polarity split using MSConvert (Kessner et
205 al., 2008). The *.mzML files were subsequently uploaded to the online collaborative research resource
206 Workflow4Metabolomics (W4M) (Guitton et al., 2017). Peak picking, grouping of chromatographic

207 peaks within and between samples, retention time alignment, and peak filling were applied through the
208 XCMS R package (Smith et al., 2006) within the LC-MS workflow of the W4M platform. In general,
209 the default parameters were applied. ‘CentWaveWith-PredIsoROIs’ was selected as the extraction
210 method for peak detection, and ‘PeakDensity’ was used for peak grouping.

211 The data matrices generated on the W4M platform were uploaded to the NOREVA platform for data
212 filtering, imputation of missing values, QC sample correction and normalization (Li et al., 2017).
213 Variables (or peak features) were considered only when they were detected in 80% of the QC samples
214 and a bias-variance tradeoff of 75% for signal correction was applied. NA values were transformed to
215 the mean value of the 'k'-neighbors found in the datasets (KNN algorithm). Batch correction was
216 performed using local polynomial fits, while normalization was achieved by applying the EigenMS
217 algorithm (Karpievitch et al., 2014). Furthermore, a time 0 centering (T0-centering) was also applied
218 as previously proposed (Narduzzi et al., 2020) to evaluate the time-trends of the variables.

219 **2.6 Statistical analysis**

220 Analysis of Variance (ANOVA)-Simultaneous Component Analysis (ASCA) was performed with the
221 MetStaT package (Smilde et al., 2005) in R environment (R Development Core Team, 2008). The
222 datasets were subsequently explored with the SIMCA-P 13.02 software (Umetrics, Umea, Sweden),
223 applying mean centering and Unit-Variance (UV) scaling to all variables. Unsupervised Principal
224 Component Analysis (PCA) and supervised (Orthogonal) Partial Least Squares-Discriminant Analysis
225 [(O)PLS-DA] were investigated as discriminant models. The validation and robustness of each model
226 were evaluated by R2X (cum), R2Y(cum) and Q2(cum) parameters, cross validation-analysis of
227 variance (CV-ANOVA), permutation tests and misclassification test. Variable Importance in
228 Projection (VIP) score greater than 1.5 was established as threshold. Additionally, heatmap analysis
229 was performed using the “heatmap.plus” package (Day, 2015), using “euclidean” as distance function
230 and “ward.D2” as clustering algorithm in R environment.

231 **2.7 Metabolite annotation**

232 First, the relevant features were compared with the CAMERA groups (Kuhl et al., 2012) obtained on
233 the W4M platform to remove possible isotopes and adduct peaks. Subsequently, tentative
234 identification was carried out by comparing the relevant features with an internal database of 500
235 metabolites analyzed under the same analytical conditions, applying an in-house developed script
236 (Narduzzi et al., 2018) for matching with a tolerance threshold of 5 ppm and 30 seconds for m/z and
237 retention time, respectively. Matches were confirmed by injection of the metabolite standards and
238 comparison of MS^2 spectra; therefore, level 1 annotation was considered for these metabolites
239 according to the confidence levels for compound annotations as recently proposed by the Compound
240 Identification work group of the Metabolomics Society (Blaženović et al., 2018). The ‘remaining’
241 features were putatively annotated by interrogating MS^2 spectra with SIRIUS 4.0 (Dührkop et al.,

242 2019). Metabolites that showed a high agreement with a single molecular structure were annotated as
243 level 2. In this sense, published literature was reviewed to consider only those molecular candidates
244 capable of explaining the biological plausibility of exposure to PCBs. Metabolites were annotated as
245 level 3 when only a probable structure could be assigned to the metabolite (e.g. molecules with a wide
246 range of possible isomers were annotated as level 3). Finally, those features with no MS/MS spectra
247 match were investigated in Metlin (Guijas et al., 2018) and HMDB (Wishart et al., 2018) to annotate
248 metabolites based simply on their accurate mass. These metabolites were annotated as level 4.
249 Furthermore, features with an accurate mass that could only provide a single chemical formula were
250 also annotated as level 4. The annotation of lipids was achieved by interrogation of MS² spectra with
251 MS-Dial ver. 4.24 (Tsugawa et al., 2020), and assigned as levels 3 to 4 after manual confirmation.

252 In addition, and to provide more confidence in the annotated metabolites, their octanol/water partition
253 coefficient (log P) was investigated to evaluate their fit in a simple linear regression curve built with
254 information from our in-house library. This was a tentative approach to exclude annotated metabolites
255 that were clearly outliers in the 'log P vs retention time' trend; therefore, their annotation was
256 probably incorrect based on the observed retention time for the related feature (Kaliszan, 1992).

257 The "Pathway Analysis module" included in the web-tool MetaboAnalyst 4.0 was used to identify the
258 metabolic pathways more affected by exposure to Aroclor 1260 according to the biomarkers of effect
259 identified (Chong et al., 2018).

260 **2.8 Bioaccumulation of PCBs caused by Aroclor 1260 exposure**

261 The bioaccumulation of DL-PCBs and NDL-PCBs in the pigs during the entire period of animal
262 experimentation was investigated by respective analysis of the 12 DL-PCBs and the 6 PCB indicators
263 (i.e. PCB28, PCB52, PCB101, PCB138, PCB153 and PCB180) in perirenal fat, which was recovered
264 in the euthanasia of the animals. The samples were analyzed by gas chromatography (GC)-HRMS
265 applying an analytical method already implemented in our laboratory (Vaccher et al., 2020). In order
266 to evaluate whether the bioaccumulation of PCBs in the perirenal fat between exposed and control
267 groups was statistically significant, F-test (for equality of variance) and T-test (for equality of means)
268 were performed in Microsoft® Excel® 2013 included in the Microsoft Office Professional Plus 2013
269 software package.

270 **3 Results**

271 **3.1 Body weight development and general observations**

272 In general, no visual observation allowed to indicate significant differences between the control and
273 exposed pigs. Animals in both groups were weighted on the same day that serum sampling was carried
274 out to monitor growth and the possible impact of PCBs exposure on it. The animals weighed 30 ± 2 kg
275 at the beginning of the experiment (D2) while they weighed 53 ± 1 kg at the end of the experiment

276 (D32). Weight gain was consistent for the experimentation period and the animal species according to
277 the animal handlers (i.e. 22 ± 2 and 23.2 ± 0.8 kg for the control and exposed animals, respectively);
278 therefore, no significant differences were observed within both groups of animals.

279 The mean concentration levels of DL-PCBs in the perirenal fat for control and exposed groups were
280 not statistically different for a 95% confidence level (i.e. 0.0915 ± 0.0007 and 0.09 ± 0.02 ng DL-
281 PCBs/kg of fat weight, respectively). On the contrary, statistical differences were observed for NDL-
282 PCBs (p -value < 0.05), with mean concentration levels of 0.3 ± 0.1 and 1.2 ± 0.1 ng NDL-PCBs/kg of
283 fat weight in the perirenal fat of control and exposed animals, respectively. In the latter case, the f-test
284 indicated that the variance for both groups was statistically equivalent. These results are in accordance
285 with our expectations, as Aroclor mixtures mainly consist of NDL-PCB congeners (98%) (Klocke and
286 Lein, 2020).

287 **3.2 LC–HRMS data**

288 Serum samples were analyzed applying traditional non-targeted LC-HRMS workflows, resulting in
289 four datasets: two datasets from metabolomics analysis of serum samples under ESI+ and ESI-
290 conditions, and another two datasets from lipidomics analysis applying both ionization conditions.
291 After data deconvolution, 1813 and 1731 features were obtained for metabolomics analysis in positive
292 and negative ionization mode, respectively. In the case of lipidomics, 3624 and 1450 features were
293 detected in ESI+ and ESI- mode, respectively.

294 After data pre-processing, metabolomics datasets (ESI+ and ESI- mode) consisted of 725 and 1731
295 variables, respectively, while 3561 and 1439 variables were contained in lipidomics datasets (ESI+
296 and ESI- mode, respectively). In general, the number of variables in the datasets corresponds to the
297 number of features detected by XCMS deconvolution, except for the metabolomics ESI+ dataset. In
298 this case, less than half of the detected features remained as variables after data pre-processing. It was
299 directly related to the fact of an observed depletion of signal intensity during batch-to-batch data
300 acquisition.

301 **3.3 General data exploration**

302 In our experimental design, two groups of animals (i.e. control and exposed pigs) and three
303 experimental stages (i.e. periods of acclimatization, exposure, and detoxification) were established. In
304 total, ten blood samples were collected per animal throughout the investigation period as indicated in
305 Figure 1, and all of these samples were included in further metabolomics studies. Since the animals in
306 both groups were under the same experimental conditions during the acclimatization and
307 detoxification stages, the samples from the datasets were divided into four different observation
308 classes for initial data exploration (i.e. ‘acclimatization’, ‘detoxification’, ‘exposed’ and ‘control’
309 groups). Neither non-supervised (i.e. PCA) nor supervised (i.e. PLS-DA) multivariate analysis

310 provided separation of the four groups. However, preliminary results showed that statistical separation
311 of groups was possible when data from the ‘detoxification’ group were included in ‘exposed’ and
312 ‘control’ groups according to the animal to which the serum sample belonged to. In this context, three
313 classes of samples belonging to ‘acclimatization’ (n = 12 observations), ‘exposed’ (n = 32) and
314 ‘control’ (n = 16) groups were established for further statistical exploration of the data.

315 Furthermore, ASCA analysis indicated that the intrinsic biological difference of each animal in our
316 experiment was one of the main sources of variance in all metabolomics and lipidomics datasets
317 (‘subject’ factor, **Table 1**). In contrast, ‘exposure’ (or not) to Aroclor 1260 was not a factor by itself
318 that explains the variance observed in the datasets. However ASCA analysis also highlighted that the
319 interaction between the ‘subject’ and ‘exposure’ factors was significant, indicating that there was a
320 subject-specific effect of the treatment.

321 To overcome the masking effect of the inter-individual variability, T0-centering was applied to all
322 datasets to address inter-individual differences and highlight differences between groups. Using
323 metabolomics data acquired under ESI- conditions as an example, **Figure 2** shows how the groups are
324 clearly separated after T0-centering when PCA is performed, while the differences between them are
325 masked before T0-centering. After T0-centering, it can be observed how the individual variability for
326 D2 and D4 is reduced; thus, leading to the grouping of samples from the acclimation period (**Figure**
327 **2.b**). A subsequent representation of the appropriate principal components on the score plot of the
328 PCA model (**Figure 2.c**) visually highlights the differences between samples based on animal biology
329 and the presence or absence of exposure to Aroclor 1260. In this case, the PCA model consisted of
330 eight principal components and while the first principal component of the model (y-axis) remarks the
331 biological differences existing in the animals of each group, the fourth principal component (x-axis)
332 highlights the differences in the samples due to exposure to Aroclor 1260. A similar pattern was
333 observed for the other datasets as indicated in Supplementary Material (**Figures S1-S3**). Applying this
334 approach, and in addition to the separation of the different groups, clustering of the samples of
335 singular individuals was also observed.

336 Significant differences in features in the datasets for the three group classes were shown in clustering
337 heatmap. **Figure 3** shows the differences observed for features detected in lipidomics analysis under
338 ESI+ conditions. This preliminary non-supervised analysis allowed to confirm the clustering of
339 samples from ‘control’, ‘exposed’ and ‘acclimatization’ groups, respectively. Furthermore, samples
340 from the same individual also clustered together except for one of the subjects from the ‘exposed’
341 group, confirming the importance of the biological status of each subject in our datasets. In addition,
342 the time factor demonstrated to not have any relevance in our datasets since no clustering from
343 samples from the sampling day was observed.

344 **3.4 Discriminant models to highlight biomarkers of effect**

345 Since the previous results showed differences in the groups due to exposure to Aroclor 1260, PLS-DA
346 models were built to highlight relevant features that could represent biomarkers of effect associated
347 with said chemical exposure. The three groups considered in our datasets were separated in all cases
348 (**Figure 4** and **Figure S4**). CV-ANOVA showed that the four PLS-DA models are statistically
349 significant (p -value < 0.05), while the values of the $R^2Y(\text{cum})$ and $Q^2Y(\text{cum})$ were always ≥ 0.649
350 and ≥ 0.405 , respectively, demonstrating the robustness of the models (**Table 2**). Permutation tests
351 consisting of 100 permutations were also carried out for each PLS-DA model and for the ‘control’ and
352 ‘exposed’ groups, confirming that the models are not the result of a random factor and that they offer a
353 valid and robust discrimination between control and exposed populations. Furthermore, a
354 misclassification test was performed on each PLS-DA model obtaining a classification accuracy
355 greater than 91.7%, with two of the four models correctly assigning the classes to all samples (**Table**
356 **2**).

357 Subsequently, VIP-plots of each PLS-DA model, including all components (2 or 3 components
358 according to the PLS-DA model) were investigated to highlight the relevant features that differentiated
359 the classes in the statistical models. Features with VIP values > 1.5 in any of the model components
360 were retained as possible biomarkers related to exposure to Aroclor 1260. In total, 129 and 276
361 features were retained from metabolomics datasets (ESI+ and ESI- conditions, respectively), while
362 589 and 240 features were retained from lipidomics datasets (ESI+ and ESI- conditions, respectively).
363 These features were considered of interest for our study since they represented the variables
364 responsible for the separation of the groups in the PLS-DA projection. These relevant features were
365 investigated against CAMERA groups to remove isotopes or adducts and considering only protonated
366 ions for subsequent metabolite annotation. Features that CAMERA noted as adducts or isotopes were
367 removed from the list of relevant features when their related protonated ions showed VIP values < 1 . If
368 their VIP values were greater than 1 for any of the model components, the adducts and isotopic
369 features were replaced by the protonated ion feature in the list of relevant features. The number of
370 aforementioned features was reduced by 11.6 and 33.6 % after relevant features selection, specifically
371 referring to the ‘metabolomics ESI+’ and ‘lipidomics ESI+’ datasets, respectively.

372 Finally, OPLS-DA models were built to confirm that the selected features differentiated the ‘control’
373 and ‘exposed’ groups and to generate S-line plots to further establish whether the annotated
374 metabolites were down- or up-regulated in pigs exposed to Aroclor 1260 (**Figures S5-S6**). The CV-
375 ANOVA of the four OPLS-DA models indicated that they are statistically significant (p -value < 0.05),
376 while $R^2Y(\text{cum})$ (> 0.94) and $Q^2(\text{cum})$ (> 0.887) parameters showed that the data fit well to the
377 models as well as their high degree of classification (**Table S1**).

378 **3.5 Metabolite annotation**

379 **Table 3** shows all the metabolites annotated as level 1 or 2, while the relevant features found by
380 metabolomics and annotated either as level 3 or 4 are included in **Tables S2-S4**. Lipids were only
381 annotated as level 3 as the maximum confidence level for the annotation due to the wide range of
382 isomeric lipids present in nature and the little structural information from our experiments for their
383 unequivocal annotation at a higher level of confidence (**Table S5-S7**).

384 Finally, in the ‘metabolomics’ datasets, 9, 24, 18, and 105 metabolites were annotated as level 1, 2, 3
385 and 4, respectively. Although metabolite annotation is time-consuming and, in general, most of the
386 relevant of features remain unidentified when performing metabolomics studies, a great effort was
387 made to annotate as many metabolites as possible. As consequence, up to 44.7 % of the features
388 observed as relevant in Section 3.4 were annotated at any of the annotation levels considered in this
389 study. In the case of ‘lipidomics’ datasets, up to 39 and 55 lipids were putatively annotated with an
390 annotation confidence level of 3 and 4, respectively. The annotated lipids represented only 16.1% of
391 the features highlighted as relevant variables in the discriminant models discussed in the previous
392 section. This highlights the main drawback of metabolomics and lipidomics approaches which is
393 metabolite annotation.

394 Biomarkers of effect, previously identified or putatively annotated, were investigated using the
395 MetaboAnalyst 4.0 pathway analysis (Chong et al., 2018), showing that lipid metabolism was
396 significantly affected by exposure to Aroclor 1260 (**Figure 5**). In this sense, for example, lipid-lipid
397 correlation analysis has shown relevant negative correlations between lysophosphatidylcholines (LPCs)
398 [i.e. LPC (16:0) and LPC (18:0)] and phosphatidylcholines (PCs) [i.e. PC (35:2) and PC (37:4)] for
399 exposed animals, which have not been observed for control animals (**Figure S7**).

400 **4. Discussion**

401 The pig was selected as an animal model due to the comparable physiology of pigs to that of humans,
402 making it an ideal model to address chemical risk assessment for human health (Goldansaz et al.,
403 2017). Both groups of animals showed similar bioaccumulation of DL-PCBs related to unknown
404 environmental and dietary exposures, while significant bioaccumulation of NDL-PCBs caused by
405 exposure to Aroclor 1260 was observed in the perirenal fat of the exposed animals compared to the
406 control group. Therefore, and in the framework of this study, the possible disturbances observed in the
407 metabolism of the pigs caused by exposure to Aroclor 1260 are attributed to NDL-PCBs.

408 The general data exploration highlighted that the inter-individual variability masks the effect of the
409 exposure to low doses of NDL-PCBs. This fact reflects one of the main risks of toxicological
410 metabolomics studies involving low doses of exposure. Chemical exposure cannot show a clear impact
411 on the metabolism because the subject variability masks the effect of the treatment. There are some
412 strategies to overcome this limitation, but given the limited number of samples, we selected the most
413 basic approach: T0-centering. This method makes it possible to follow the fate of the variables over

414 time. Thus, if the fate of the variables varies in the different groups (control vs. exposed), it means that
415 there is a difference in their metabolism between them. The results clearly show that this approach
416 highlighted several features with a different fate between the groups, indicating a change in their
417 metabolism due to the exposure to Aroclor 1260.

418 Our study is a first approach to evaluate the consequences of exposure to NDL-PCBs in pigs at
419 realistic exposure levels (in the order of few ng/kg b.w. per day), at which no observable toxicity is
420 expected. There was great uncertainty at the time of planning the animal experimentation as to
421 whether the metabolism of pigs would be altered by such low levels of exposure to NDL-PCBs or if
422 these alterations would have any toxicological relevance, while the selection of a greater number of
423 animals for this first approach was not exempt of greater economical and ethical costs. In this sense,
424 current ethical standards in animal experimentation require replacing, refining and reducing the use of
425 animals in scientific research and testing as much as possible (3R principles) (Scholz et al., 2013). In
426 this context where only six animals were included in the animal experiment. We preferred to
427 unbalance the experiment towards the exposed group to reduce the odds of missing biomarkers
428 (reduce the false negative ratio). Certain limitations can be attributed to the present study due to the
429 low number of animals included in the experimentation which might undermine the validity of the
430 biomarkers found. Therefore, as discussed below, the main results obtained in our study have been
431 compared to previous toxicological and epidemiological studies that include a greater number of
432 individuals under study to give a biological explanation of the biomarkers, strengthening their validity.
433 Nevertheless, we are aware that a complete validation will require further experimentation to confirm
434 or discard these biomarkers. Indeed, taken singularly, none of the metabolic markers identified in this
435 experiment are unique to Aroclor 1260 exposure. The strength of this experimentation is the fact that,
436 through a multi-marker approach, it was possible to identify a metabolic profile uncommon in young
437 pigs, which is generally associated with long-term disease development. This study demonstrates that
438 such risks of disease development are associated with environmental exposure to chemicals as NDL-
439 PCBs at low doses, as discussed below. Linoleic acid metabolism, glycerophospholipid metabolism,
440 and arachidonic acid metabolism were the metabolic pathways more impacted by this chemical
441 exposure.

442 PCB exposure has previously been associated with glucose and lipid metabolic disorders in the liver,
443 which can lead to chronic systemic metabolic disorders such as obesity, type 2 diabetes, fatty liver
444 disease, cardiovascular disease, and cancer (Shan et al., 2020). Serum lipids have also been shown to
445 be disturbed by PCB exposure, causing dysregulation of cholesterol synthesis and degradation
446 mechanisms (Hennig et al., 2005). Among the lipids tentatively annotated in this work,
447 glycerophospholipids and specifically glycerophosphocolines and glycerophosphoethanolamines,
448 which are involved in lipid metabolism and regulation, are the main classes of lipids disturbed by
449 exposure to NDL-PCBs. Previous research has already shown disturbances in glycerophospholipid

450 levels in serum and plasma samples from humans exposed to POPs, including PCBs (Carrizo et al.,
451 2017)(Walker et al., 2019). Glycerophospholipids are involved in the formation of the cellular
452 membranes of all organisms and organelles within cells, as well as in cell signaling systems and as an
453 anchor for proteins in cell membranes. They are also involved in the transport of triacylglycerols and
454 cholesterol in the body (Blanco and Blanco, 2017)(Carrizo et al., 2017)(Triebel, 2019). Important
455 metabolome alterations, mainly related to glycerophospholipid levels in serum, have recently been
456 reported in rat offspring after in utero and lactational exposure to PCB 180, which is a NDL-PCB
457 congener and one of the most abundant in the environment (Pikkarainen et al., 2019). Furthermore, a
458 generalized increase in glycerophospholipid levels has also been observed in rat pheochromocytoma
459 PC12 cells exposed to PCB 153, which is also a NDL-PCB congener (Wang et al., 2019).

460 Within the group of glycerophosphocolines, and as observed in our study, it has been found that LPCs
461 are the main biomarkers of effect in the serum of mice exposed to diethylhexylphthalate (DEHP) and
462 Aroclor 1254 at doses higher than environmental exposure levels (Zhang et al., 2012). Either in mice
463 (Zhang et al., 2012) or in pigs (as shown in this work), animals exposed to Aroclor mixtures show
464 increased concentration levels of LPC (16:0) and LPC (18:0) in serum in comparison to control
465 individuals. Increased plasma levels of LPCs are related to cardiovascular diseases, diabetes, ovarian
466 cancer, and renal failure (Law et al., 2019). These findings indicating an impact on LPC levels
467 associated with NDL-PCB exposure are in line with previous studies. They have linked
468 cardiometabolic diseases and exposure to endocrine disrupting compounds, such as PCBs, where LPC
469 metabolites have been suggested as mediators in those events (Salihovic et al., 2016). LPCs result
470 from the cleavage of PCs through the action of phospholipase A2 (PLA2) and/or by the transfer of
471 fatty acids to free cholesterol through lecithin-cholesterol acyltransferase. LPCs can be converted back
472 into PCs by the action of the enzyme lysophosphatidylcholine acyltransferase in the presence of Acyl-
473 CoA (Law et al., 2019). These metabolic processes are part of the Lands' cycle, which in addition to
474 the Kennedy pathway and the phosphatidylethanolamine N-methyltransferase pathway constitute the
475 synthesis pathways of PCs (Moessinger et al., 2014). In this framework, the negative correlations
476 between LPC (16:0) and LPC (18:0) with PC (35:2) and PC (37:4) for exposed animals indicate a
477 probable disturbance of the Lands' cycle. This hypothesis is also supported by the identification at
478 level 1 of arachidonic acid as a biomarker of effect of exposure to NDL-PCBs. Furthermore, in the
479 present work, several sphingomyelins, which belong to the sphingolipid class, have also been
480 determined as potential effect biomarkers of Aroclor 1260 exposure. Sphingomyelins also participate
481 in PLA2 activity (Rodriguez-Cuenca et al., 2017), which reinforces our hypothesis on the alteration of
482 Lands' cycle caused by exposure to NDL-PCBs at environmental dose levels.

483 As mentioned above, PLA2s hydrolyze the sn-2 ester bond of cellular phospholipids, producing LPCs
484 and free fatty acids, frequently arachidonic acid, which is the precursor to the eicosanoid family of
485 potent inflammatory mediators (Balsinde et al., 2002). Activation of PLA2s and increased arachidonic

486 acid levels caused by exposure to NDL-PCBs have also been previously reported in rat cells and
487 human platelets (Brant and Caruso, 2006)(Forsell et al., 2005). Increased levels of arachidonic acid are
488 associated with inflammatory processes that, even at low-grade levels, can induce metabolic and
489 cardiovascular diseases (Sonnweber et al., 2018). Free arachidonic acid also induces oxidative stress,
490 which is a relevant factor in the development of hepatic steatosis (Sonnweber et al., 2018). Hepatic
491 steatosis is an hepatic disorder that can lead to the development of nonalcoholic fatty liver disease,
492 which has previously been associated with exposure to NDL-PCBs (Wahlang et al., 2019). The
493 hepatotoxicity of Aroclor 1260 mixture and the link between exposure to it and nonalcoholic fatty
494 liver disease progression have been previously documented (Armstrong and Guo, 2019). Although it is
495 not yet clear, oxidative stress may be the key link between nonalcoholic fatty liver disease and
496 cardiovascular disease (Polimeni et al., 2015). The alteration of the linolenic acid pathway represents
497 another evidence of oxidative stress caused by exposure to PCBs. Bioactive oxidized linoleic acid
498 metabolites and diols of linoleate epoxides have previously been linked to oxidative stress and
499 inflammatory disorders (Deng et al., 2019).

500 In addition, several ether-linked phosphatidylcholines and ether-linked phosphatidylethanolamine
501 were found as biomarkers of effect in the serum of pigs exposed to Aroclor 1260. In contrast to LPCs,
502 a general decrease of ether lipid levels was observed in the serum of exposed animals compared to the
503 control animals. Recently, ether lipids have been proposed as potential biomarkers of various diseases,
504 linking decreased ether lipid synthesis with multiple neurological and metabolic abnormalities (Dean
505 and Lodhi, 2018). However, it is not yet clear whether they are simply by-products of disease
506 processes or whether they contribute to disease pathogenesis. Decreased levels of ether-phospholipids
507 in the liver have also been observed in rats exposed to different doses of a DL-PCB, specifically PCB
508 126, and which have been related to hepatic disorders (Kania-Korwel et al., 2017). In this sense,
509 although DL-PCBs and NDL-PCBs have been shown to have different mechanisms of action in liver
510 diseases such as nonalcoholic fatty liver disease, they share common effects (Wahlang et al., 2019).

511 Although all these results show a significant impact on lipid metabolism caused by exposure to NDL-
512 PCBs, other identified biomarkers of effect indicate an alteration of other metabolic pathways. Several
513 metabolites from the kynurenine pathway of tryptophan metabolism have been identified as effect
514 biomarkers of Aroclor 1260 exposure, namely L-tryptophan, kynurenine, quinaldic acid and N'-
515 formylkynurenine. Previous *in vivo* and *in vitro* studies have shown an impact of Aroclor 1254
516 mixture and PCB3, which is a NDL-PCB congener, on tryptophan metabolism (Khan and Thomas,
517 2004)(Zhang et al., 2012)(Zhang et al., 2021). Similar evidences have been reported for exposure to
518 DL-PCBs (Mesnage et al., 2018). The disturbance of tryptophan-kynurenine pathway is related to
519 inflammation, oxidative stress and immune activation in cardiovascular diseases (Wang et al., 2015).
520 This finding agrees with the previous discussion about abnormal lipid metabolism caused by exposure
521 to Aroclor 1260, which is another metabolic indicator of the pathogenesis of cardiovascular disease.

522 Indeed, there are several pieces of evidence linking chemical exposure to PCBs and the development
523 of cardiovascular diseases (Perkins et al., 2016). In this sense, this work provides new evidence that
524 current environmental exposures to NDL-PCBs can cause health effects similar to those previously
525 observed in toxicological studies at higher exposure doses but likely to be observed after a longer
526 period of exposure. Therefore, although levels of exposure to PCBs have been reduced in recent
527 decades (Lehmann et al., 2015), the observed metabolic changes caused by exposure to Aroclor 1260
528 suggest that actual exposure scenarios to NDL-PCBs contribute to the onset and progression of
529 environmental diseases, namely cardiovascular disease.

530 **5 Concluding remarks**

531 This study provides new information on biomarkers of effect in serum samples associated with
532 exposure to Aroclor 1260 at dietary dose levels (i.e. 6.1 ng of six NDL-PCBs/kg b.w. per day). By
533 extension, these biomarkers of effect have been related to exposure to NDL-PCBs, which have been
534 shown to bioaccumulate in perirenal fat. In addition, the investigation of the pig as an animal model
535 for the hazard identification of NDL-PCBs gives new evidence for the human health risk assessment
536 of NDL-PCBs. Our no hypothesis-driven approach has demonstrated to be suitable to highlight the
537 biomarkers of effect related to exposure to NDL-PCBs at levels of environmental exposure. Several
538 glycerophosphocholines, some fatty acids, including arachidonic acid and linolenic acid, tryptophan,
539 kynurenine and some of its metabolites, have been found as probable biomarkers of effect of said
540 chemical exposure. These metabolites are mainly associated with glycerophospholipids metabolism,
541 fatty acid metabolism and tryptophan-kynurenine pathway; thus, these metabolic pathways have been
542 identified as the main pathways impacted by exposure to NDL-PCBs at low dose levels. Such
543 metabolic alterations induce chronic oxidative stress and inflammation that are important factors in
544 cardiovascular disease. These observations agree with other toxicological and epidemiological studies
545 and suggest that exposure to current low levels of NDL-PCBs may still cause adverse health effects.

546 **Acknowledgments:** This project has received funding from the European Union's Horizon 2020
547 research and innovation programme under the Marie Skłodowska-Curie grant agreement
548 HAZARDOMics No 795946.

549 **References:**

- 550 AFSSA, 2007. AVIS de l'AFSSA relatif à l'établissement de teneurs maximales pertinentes en
551 polychlorobiphényles qui ne sont pas de type dioxine (PCB « non dioxin-like », PCB-NDL) dans
552 divers aliments. Agence Française Sécurité Sanit. des Aliment. 1–28.
- 553 Alarcón, S., Esteban, J., Roos, R., Heikkinen, P., Sánchez-Pérez, I., Adamsson, A., Toppari, J.,
554 Koskela, A., Finnilä, M.A.J., Tuukkanen, J., Herlin, M., Hamscher, G., Leslie, H.A.,
555 Korkalainen, M., Halldin, K., Schrenk, D., Håkansson, H., Viluksela, M., 2021. Endocrine,
556 metabolic and apical effects of in utero and lactational exposure to non-dioxin-like
557 2,2',3,4,4',5,5'-heptachlorobiphenyl (PCB 180): A postnatal follow-up study in rats. *Reprod.*
558 *Toxicol.* 102, 109–127. <https://doi.org/10.1016/j.reprotox.2021.04.004>
- 559 Armstrong, L.E., Guo, G.L., 2019. Understanding Environmental Contaminants' Direct Effects on

560 Non-alcoholic Fatty Liver Disease Progression. *Curr. Environ. Heal. reports* 6, 95–104.
561 <https://doi.org/10.1007/s40572-019-00231-x>

562 Balsinde, J., Winstead, M. V., Dennis, E.A., 2002. Phospholipase A2 regulation of arachidonic acid
563 mobilization. *FEBS Lett.* 531, 2–6. [https://doi.org/10.1016/S0014-5793\(02\)03413-0](https://doi.org/10.1016/S0014-5793(02)03413-0)

564 Blanco, A., Blanco, G., 2017. Chapter 5 - Lipids, in: Blanco, A., Blanco, G. (Eds.), *Medical*
565 *Biochemistry*. Academic Press, pp. 99–119. [https://doi.org/10.1016/B978-0-12-803550-4/00005-](https://doi.org/10.1016/B978-0-12-803550-4/00005-7)
566 7

567 Blaženović, I., Kind, T., Ji, J., Fiehn, O., 2018. Software tools and approaches for compound
568 identification of LC-MS/MS data in metabolomics. *Metabolites* 8.
569 <https://doi.org/10.3390/metabo8020031>

570 Brant, K.A., Caruso, R.L., 2006. PCB 50 stimulates release of arachidonic acid and prostaglandins
571 from late gestation rat amnion fibroblast cells. *Reprod. Toxicol.* 22, 591–598.
572 <https://doi.org/10.1016/j.reprotox.2006.04.012>

573 Carlsson, P., Breivik, K., Brorström-Lundén, E., Cousins, I., Christensen, J., Grimalt, J.O., Halsall, C.,
574 Kallenborn, R., Abass, K., Lammel, G., Munthe, J., Macleod, M., Odland, J.Ø., Pawlak, J.,
575 Rautio, A., Reiersen, L.-O., Schlabach, M., Stemmler, I., Wilson, S., Henry, &, 2018.
576 Polychlorinated biphenyls (PCBs) as sentinels for the elucidation of Arctic environmental change
577 processes: a comprehensive review combined with ArcRisk project results. *Environ. Sci. Pollut.*
578 *Res.* 25, 22499–22528. <https://doi.org/10.1007/s11356-018-2625-7>

579 Carrizo, D., Chevallier, O.P., Woodside, J. V., Brennan, S.F., Cantwell, M.M., Cuskelly, G., Elliott,
580 C.T., 2017. Untargeted metabolomic analysis of human serum samples associated with exposure
581 levels of Persistent organic pollutants indicate important perturbations in Sphingolipids and
582 Glycerophospholipids levels. *Chemosphere* 168, 731–738.
583 <https://doi.org/10.1016/j.chemosphere.2016.11.001>

584 Chong, J., Soufan, O., Li, C., Caraus, I., Li, S., Bourque, G., Wishart, D.S., Xia, J., 2018.
585 MetaboAnalyst 4.0: Towards more transparent and integrative metabolomics analysis. *Nucleic*
586 *Acids Res.* 46, W486–W494. <https://doi.org/10.1093/nar/gky310>

587 Christensen, K., Carlson, L.M., Lehmann, G.M., 2021. The role of epidemiology studies in human
588 health risk assessment of polychlorinated biphenyls. *Environ. Res.* 194, 110662.
589 <https://doi.org/10.1016/j.envres.2020.110662>

590 Dai, Y., Huo, X., Cheng, Z., Faas, M.M., Xu, X., 2020. Early-life exposure to widespread
591 environmental toxicants and maternal-fetal health risk: A focus on metabolomic biomarkers. *Sci.*
592 *Total Environ.* 739, 139626. <https://doi.org/10.1016/j.scitotenv.2020.139626>

593 Day, A., 2015. Package “heatmap.plus” - Heatmap with more sensible behavior.

594 Dean, J.M., Lodhi, I.J., 2018. Structural and functional roles of ether lipids. *Protein Cell* 9, 196–206.
595 <https://doi.org/10.1007/s13238-017-0423-5>

596 Deng, P., Barney, J., Petriello, M.C., Morris, A.J., Wahlang, B., Hennig, B., 2019. Hepatic
597 metabolomics reveals that liver injury increases PCB 126-induced oxidative stress and metabolic
598 dysfunction. *Chemosphere* 217, 140–149. <https://doi.org/10.1016/j.chemosphere.2018.10.196>

599 Dührkop, K., Fleischauer, M., Ludwig, M., Aksenov, A.A., Melnik, A. V., Meusel, M., Dorrestein,
600 P.C., Rousu, J., Böcker, S., 2019. SIRIUS 4: a rapid tool for turning tandem mass spectra into
601 metabolite structure information. *Nat. Methods* 16, 299–302. [https://doi.org/10.1038/s41592-](https://doi.org/10.1038/s41592-019-0344-8)
602 019-0344-8

603 EFSA, 2014. Modern methodologies and tools for human hazard assessment of chemicals. *EFSA J.*
604 12, 1–87. <https://doi.org/10.2903/j.efsa.2014.3638>

605 EFSA, 2005. Opinion of the Scientific Panel on contaminants in the food chain [CONTAM] related to
606 the presence of non dioxin-like polychlorinated biphenyls (PCB) in feed and food. *EFSA J.* 284,
607 1–137.

608 Faroon, O.M., Keith, L.S., Smith-Simon, C., De Rosa, C.T., 2003. Polychlorinated biphenyls : Human
609 health aspects, in: *Concise International Chemical Assessment Document 55*. World Health
610 Organization, Geneva (Switzerland).

611 Forsell, P.K.A., Olsson, A.O., Andersson, E., Nallan, L., Gelb, M.H., 2005. Polychlorinated biphenyls
612 induce arachidonic acid release in human platelets in a tamoxifen sensitive manner via activation
613 of group IVA cytosolic phospholipase A2- α . *Biochem. Pharmacol.* 71, 144–155.
614 <https://doi.org/10.1016/j.bcp.2005.10.014>

615 Goldansaz, S.A., Guo, A.C., Sajed, T., Steele, M.A., Plastow, G.S., Wishart, D.S., 2017. Livestock
616 metabolomics and the livestock metabolome: A systematic review. *PLoS One* 12, 1–26.
617 <https://doi.org/10.1371/journal.pone.0177675>

618 Grimm, F.A., Hu, D., Kania-Korwel, I., Lehmler, H.J., Ludewig, G., Hornbuckle, K.C., Duffel, M.W.,
619 Bergman, Å., Robertson, L.W., 2015. Metabolism and metabolites of polychlorinated biphenyls.
620 *Crit. Rev. Toxicol.* 45, 245–272. <https://doi.org/10.3109/10408444.2014.999365>

621 Guijas, C., Montenegro-burke, J.R., Domingo-almenara, X., Palermo, A., Warth, B., Hermann, G.,
622 Koellensperger, G., Huan, T., Uritboonthai, W., Aisporna, A.E., Wolan, D.W., Spilker, M.E.,
623 Benton, H.P., Siuzdak, G., 2018. METLIN: A Technology Platform for Identifying Knowns and
624 Unknowns. *Anal. Chem.* 90, 3156–3164. <https://doi.org/10.1021/acs.analchem.7b04424>

625 Guitton, Y., Tremblay-Franco, M., Le Corguillé, G., Martin, J.F., Pétéra, M., Roger-Mele, P.,
626 Delabrière, A., Goulitquer, S., Monsoor, M., Duperier, C., Canlet, C., Servien, R., Tardivel, P.,
627 Caron, C., Giacomoni, F., Thévenot, E.A., 2017. Create, run, share, publish, and reference your
628 LC–MS, FIA–MS, GC–MS, and NMR data analysis workflows with the
629 Workflow4Metabolomics 3.0 Galaxy online infrastructure for metabolomics. *Int. J. Biochem.*
630 *Cell Biol.* 93, 89–101. <https://doi.org/10.1016/j.biocel.2017.07.002>

631 Heindel, J.J., Blumberg, B., Cave, M., Machtinger, R., Mantovani, A., Mendez, M.A., Nadal, A.,
632 Palanza, P., Panzica, G., Sargis, R., Vandenberg, L.N., vom Saal, F., 2017. Metabolism
633 disrupting chemicals and metabolic disorders. *Reprod. Toxicol.* 68, 3–33.
634 <https://doi.org/10.1016/j.reprotox.2016.10.001>

635 Hennig, B., Reiterer, G., Toborek, M., Matveev, S. V., Daugherty, A., Smart, E., Robertson, L.W.,
636 2005. Dietary fat interacts with PCBs to induce changes in lipid metabolism in mice deficient in
637 low-density lipoprotein receptor. *Environ. Health Perspect.* 113, 83–87.
638 <https://doi.org/10.1289/ehp.7280>

639 Hernández-Mesa, M., Le Bizec, B., Dervilly, G., 2021. Metabolomics in chemical risk analysis – A
640 review. *Anal. Chim. Acta* 1154. <https://doi.org/10.1016/j.aca.2021.338298>

641 Hulin, M., Sirot, V., Vasseur, P., Mahe, A., Leblanc, J.C., Jean, J., Marchand, P., Venisseau, A., Le
642 Bizec, B., Rivière, G., 2020. Health risk assessment to dioxins, furans and PCBs in young
643 children: The first French evaluation. *Food Chem. Toxicol.* 139, 111292.
644 <https://doi.org/10.1016/j.fct.2020.111292>

645 IARC, W.G. on the E. of C.R. to H., 2016. Polychlorinated Biphenyls and Polybrominated Biphenyls,
646 IARC monographs on the evaluation of carcinogenic risks to humans. International Agency for
647 Research on Cancer (IARC), Lyon (France).

648 JECFA, 2016. Safety evaluation of certain food additives and contaminants Non-dioxin-like
649 polychlorinated biphenyls. Suppl. 1 Non-Dioxin-Like Polychlorinated Biphenyls / Prep. by
650 Eightieth Meet. Jt. FAO/WHO Expert Comm. Food Addit. (JECFA). *WHO Food Addit.* 71-S1,
651 1–431.

652 Kaliszan, R., 1992. Quantitative structure –(chromatographic) retention relationships. *Anal. Chem.*
653 64, 619–631. <https://doi.org/10.1016/j.chroma.2007.03.108>

654 Kania-Korwel, I., Wu, X., Wang, K., Lehmler, H.J., 2017. Identification of lipidomic markers of
655 chronic 3,3',4,4',5-pentachlorobiphenyl (PCB 126) exposure in the male rat liver. *Toxicology*
656 390, 124–134. <https://doi.org/10.1016/j.tox.2017.09.005>

657 Karpievitch, Y. V., Nikolic, S.B., Wilson, R., Sharman, J.E., Edwards, L.M., 2014. Metabolomics data
658 normalization with EigenMS. *PLoS One* 9, 1–10. <https://doi.org/10.1371/journal.pone.0116221>

659 Kessner, D., Chambers, M., Burke, R., Agus, D., Mallick, P., 2008. ProteoWizard: Open source
660 software for rapid proteomics tools development. *Bioinformatics* 24, 2534–2536.
661 <https://doi.org/10.1093/bioinformatics/btn323>

662 Khan, I.A., Thomas, P., 2004. Aroclor 1254 inhibits tryptophan hydroxylase activity in rat brain. *Arch.*
663 *Toxicol.* 78, 316–320. <https://doi.org/10.1007/s00204-003-0540-1>

664 Kim, J.T., Choi, Y.J., Barghi, M., Kim, J.H., Jung, J.W., Kim, K., Kang, J.H., Lammel, G., Chang,
665 Y.S., 2021. Occurrence, distribution, and bioaccumulation of new and legacy persistent organic
666 pollutants in an ecosystem on King George Island, maritime Antarctica. *J. Hazard. Mater.* 405,
667 124141. <https://doi.org/10.1016/j.jhazmat.2020.124141>

668 Klocke, C., Lein, P.J., 2020. Evidence implicating non-dioxin-like congeners as the key mediators of
669 polychlorinated biphenyl (Pcb) developmental neurotoxicity. *Int. J. Mol. Sci.* 21.

670 <https://doi.org/10.3390/ijms21031013>

671 Kuhl, C., Tautenhahn, R., Bo, C., Larson, T.R., Neumann, S., 2012. CAMERA: An Integrated
672 Strategy for Compound Spectra Extraction and Annotation of Liquid Chromatography/Mass
673 Spectrometry Data Sets. *Anal. Chem.* 84, 283–289. <https://doi.org/10.1021/ac202450g>

674 Law, S.H., Chan, M.L., Marathe, G.K., Parveen, F., Chen, C.H., Ke, L.Y., 2019. An updated review of
675 lysophosphatidylcholine metabolism in human diseases. *Int. J. Mol. Sci.* 20, 1–24.
676 <https://doi.org/10.3390/ijms20051149>

677 Lehmann, G.M., Christensen, K., Maddaloni, M., Phillips, L.J., 2015. Evaluating health risks from
678 inhaled polychlorinated biphenyls: Research needs for addressing uncertainty. *Environ. Health*
679 *Perspect.* 123, 109–113. <https://doi.org/10.1289/ehp.1408564>

680 Li, B., Tang, J., Yang, Q., Li, S., Cui, X., Li, Y., Chen, Y., WeiweiXue, Li, X., Zhu, F., 2017.
681 NOREVA: normalization and evaluation of MS-based metabolomics data. *Nucleic Acids Res.*
682 45, 162–170.

683 Lim, J.J., Li, X., Lehmler, H.J., Wang, D., Gu, H., Cui, J.Y., 2020. Gut Microbiome Critically Impacts
684 PCB-induced Changes in Metabolic Fingerprints and the Hepatic Transcriptome in Mice.
685 *Toxicol. Sci.* 177, 168–187. <https://doi.org/10.1093/toxsci/kfaa090>

686 Marchand, J., Guitton, Y., Martineau, E., Royer, A.L., Balgoma, D., Bizec, B. Le, Giraudeau, P.,
687 Dervilly, G., 2021. Extending the lipidome coverage by combining different mass spectrometric
688 platforms: An innovative strategy to answer chemical food safety issues. *Foods* 10.
689 <https://doi.org/10.3390/foods10061218>

690 Mesnage, R., Biserni, M., Balu, S., Frainay, C., Poupin, N., Jourdan, F., Wozniak, E., Xenakis, T.,
691 Mein, C.A., Antoniou, M.N., 2018. Integrated transcriptomics and metabolomics reveal
692 signatures of lipid metabolism dysregulation in HepaRG liver cells exposed to PCB 126. *Arch.*
693 *Toxicol.* 92, 2533–2547. <https://doi.org/10.1007/s00204-018-2235-7>

694 Moessinger, C., Klizaite, K., Steinhagen, A., Philippou-Massier, J., Shevchenko, A., Hoch, M., Ejsing,
695 C.S., Thiele, C., 2014. Two different pathways of phosphatidylcholine synthesis, the Kennedy
696 Pathway and the Lands Cycle, differentially regulate cellular triacylglycerol storage. *BMC Cell*
697 *Biol.* 15, 1–17. <https://doi.org/10.1186/s12860-014-0043-3>

698 Narduzzi, L., Dervilly, G., Marchand, A., Audran, M., Le Bizec, B., Buisson, C., 2020. Applying
699 metabolomics to detect growth hormone administration in athletes: Proof of concept. *Drug Test.*
700 *Anal.* 12, 887–899. <https://doi.org/10.1002/dta.2798>

701 Narduzzi, L., Stanstrup, J., Mattivi, F., Franceschi, P., 2018. The compound characteristics
702 comparison (Ccc) approach: A tool for improving confidence in natural compound identification.
703 *Food Addit. Contam. - Part A Chem. Anal. Control. Expo. Risk Assess.* 35, 2145–2157.
704 <https://doi.org/10.1080/19440049.2018.1523572>

705 Olesti, E., González-Ruiz, V., Wilks, M.F., Bocard, J., Rudaz, S., 2021. Approaches in metabolomics
706 for regulatory toxicology applications. *Analyst* 146, 1820–1834.
707 <https://doi.org/10.1039/d0an02212h>

708 Orešič, M., McGlinchey, A., Wheelock, C.E., Hyötyläinen, T., 2020. Metabolic signatures of the
709 exposome—quantifying the impact of exposure to environmental chemicals on human health.
710 *Metabolites* 10, 1–31. <https://doi.org/10.3390/metabo10110454>

711 Peng, T., Royer, A.L., Guitton, Y., Le Bizec, B., Dervilly-Pinel, G., 2017. Serum-based metabolomics
712 characterization of pigs treated with ractopamine. *Metabolomics* 13, 1–15.
713 <https://doi.org/10.1007/s11306-017-1212-0>

714 Perkins, J.T., Petriello, M.C., Newsome, B.J., Hennig, B., 2016. Polychlorinated biphenyls and links
715 to cardiovascular disease. *Environ. Sci. Pollut. Res.* 23, 2160–2172.
716 <https://doi.org/10.1007/s11356-015-4479-6>

717 Petriello, M.C., Hoffman, J.B., Vsevolozhskaya, O., Morris, A.J., Hennig, B., 2018. Dioxin-like PCB
718 126 increases intestinal inflammation and disrupts gut microbiota and metabolic homeostasis.
719 *Environ. Pollut.* 242, 1022–1032. <https://doi.org/10.1016/j.envpol.2018.07.039>

720 Pielaat, A., Barker, G.C., Hendriksen, P., Hollman, P., Peijnenburg, A., Ter Kuile, B.H., 2013. A
721 foresight study on emerging technologies: State of the art of omics technologies and potential
722 applications in food and feed safety. REPORT 1: Review on the state of art of omics
723 technologies in risk assessment related to food and feed safety. *EFSA Support. Inf.* EN-495, 1–
724 126.

725 Pikkarainen, A., Lehtonen, M., Håkansson, H., Auriola, S., Viluksela, M., 2019. Gender- and dose-
726 related metabolome alterations in rat offspring after in utero and lactational exposure to PCB
727 180. *Toxicol. Appl. Pharmacol.* 370, 56–64. <https://doi.org/10.1016/j.taap.2019.03.013>

728 Polimeni, L., del Ben, M., Baratta, F., Perri, L., Albanese, F., Pastori, D., Violi, F., Angelico, F., 2015.
729 Oxidative stress: New insights on the association of nonalcoholic fatty liver disease and
730 atherosclerosis. *World J. Hepatol.* 7, 1325–1336. <https://doi.org/10.4254/wjh.v7.i10.1325>

731 R Development Core Team, 2008. A language and environment for statistical computing. R
732 Foundation for Statistical Computing [WWW Document]. Vienna, Austria. ISBN 3-900051-07-
733 0.

734 Rodriguez-Cuenca, S., Pellegrinelli, V., Campbell, M., Oresic, M., Vidal-Puig, A., 2017.
735 Sphingolipids and glycerophospholipids – The “ying and yang” of lipotoxicity in metabolic
736 diseases. *Prog. Lipid Res.* 66, 14–29. <https://doi.org/10.1016/j.plipres.2017.01.002>

737 Rushneck, D.R., Beliveau, A., Fowler, B., Hamilton, C., Hoover, D., Kaye, K., Berg, M., Smith, T.,
738 Telliard, W.A., Roman, H., Ruder, E., Ryan, L., 2004. Concentrations of dioxin-like PCB
739 congeners in unweathered Aroclors by HRGC/HRMS using EPA Method 1668A. *Chemosphere*
740 54, 79–87. [https://doi.org/10.1016/S0045-6535\(03\)00664-7](https://doi.org/10.1016/S0045-6535(03)00664-7)

741 Salihovic, S., Ganna, A., Fall, T., Broeckling, C.D., Prenni, J.E., van Bavel, B., Lind, P.M., Ingelsson,
742 E., Lind, L., 2016. The metabolic fingerprint of p,p'-DDE and HCB exposure in humans.
743 *Environ. Int.* 88, 60–66. <https://doi.org/10.1016/j.envint.2015.12.015>

744 Scholz, S., Sela, E., Blaha, L., Braunbeck, T., Galay-Burgos, M., García-Franco, M., Guinea, J.,
745 Klüver, N., Schirmer, K., Tanneberger, K., Tobor-Kapłon, M., Witters, H., Belanger, S.,
746 Benfenati, E., Creton, S., Cronin, M.T.D., Eggen, R.I.L., Embry, M., Ekman, D., Gourmelon, A.,
747 Halder, M., Hardy, B., Hartung, T., Hubesch, B., Jungmann, D., Lampi, M.A., Lee, L., Léonard,
748 M., Küster, E., Lillicrap, A., Luckenbach, T., Murk, A.J., Navas, J.M., Peijnenburg, W., Repetto,
749 G., Salinas, E., Schüürmann, G., Spielmann, H., Tollefsen, K.E., Walter-Rohde, S., Whale, G.,
750 Wheeler, J.R., Winter, M.J., 2013. A European perspective on alternatives to animal testing for
751 environmental hazard identification and risk assessment. *Regul. Toxicol. Pharmacol.* 67, 506–
752 530. <https://doi.org/10.1016/j.yrtph.2013.10.003>

753 Shan, Q., Li, H., Chen, N., Qu, F., Guo, J., 2020. Understanding the multiple effects of PCBs on lipid
754 metabolism. *Diabetes, Metab. Syndr. Obes. Targets Ther.* 13, 3691–3702.
755 <https://doi.org/10.2147/DMSO.S264851>

756 Shi, X., Wahlang, B., Wei, X., Yin, X., Falkner, K.C., Prough, R.A., Kim, S.H., Mueller, E.G.,
757 McClain, C.J., Cave, M., Zhang, X., 2012. Metabolomic analysis of the effects of
758 polychlorinated biphenyls in nonalcoholic fatty liver disease. *J. Proteome Res.* 11, 3805–3815.
759 <https://doi.org/10.1021/pr300297z>

760 Simon, T.W., Simons, S.S., Preston, R.J., Boobis, A.R., Cohen, S.M., Doerrer, N.G., Fenner-Crisp,
761 P.A., McMullin, T.S., Mcqueen, C.A., Rowlands, C.J., 2014. The use of mode of action
762 information in risk assessment: Quantitative key events/dose-response framework for modeling
763 the dose-response for key events. *Crit. Rev. Toxicol.* 44, 17–43.
764 <https://doi.org/10.3109/10408444.2014.931925>

765 Sirot, V., Tard, A., Venisseau, A., Brosseau, A., Marchand, P., Le Bizec, B., Leblanc, J.C., 2012.
766 Dietary exposure to polychlorinated dibenzo-p-dioxins, polychlorinated dibenzofurans and
767 polychlorinated biphenyls of the French population: Results of the second French Total Diet
768 Study. *Chemosphere* 88, 492–500. <https://doi.org/10.1016/j.chemosphere.2012.03.004>

769 Smilde, A.K., Jansen, J.J., Hoefsloot, H.C.J., Lamers, R.J.A.N., van der Greef, J., Timmerman, M.E.,
770 2005. ANOVA-simultaneous component analysis (ASCA): A new tool for analyzing designed
771 metabolomics data. *Bioinformatics* 21, 3043–3048. <https://doi.org/10.1093/bioinformatics/bti476>

772 Smith, C. a, Want, E.J., O’Maille, G., Abagyan, R., Siuzdak, G., 2006. XCMS: processing mass
773 spectrometry data for metabolite profiling using nonlinear peak alignment, matching, and
774 identification. *Anal. Chem.* 78, 779–87. <https://doi.org/10.1021/ac051437y>

775 Sonnweber, T., Pizzini, A., Nairz, M., Weiss, G., Tancevski, I., 2018. Arachidonic acid metabolites in
776 cardiovascular and metabolic diseases. *Int. J. Mol. Sci.* 19. <https://doi.org/10.3390/ijms19113285>

777 Triebl, A., 2019. Encyclopedia of Lipidomics. *Encycl. Lipidomics.* <https://doi.org/10.1007/978-94-007-7864-1>

778
779 Tsugawa, H., Ikeda, K., Takahashi, M., Satoh, A., Mori, Y., Uchino, H., Okahashi, N., Yamada, Y.,

780 Tada, I., Bonini, P., Higashi, Y., Okazaki, Y., Zhou, Z., Zhu, Z.J., Koelmel, J., Cajka, T., Fiehn,
781 O., Saito, K., Arita, Masanori, Arita, Makoto, 2020. A lipidome atlas in MS-DIAL 4. *Nat.*
782 *Biotechnol.* 38, 1159–1163. <https://doi.org/10.1038/s41587-020-0531-2>

783 Ulbrich, B., Stahlmann, R., 2004. Developmental toxicity of polychlorinated biphenyls (PCBs): A
784 systematic review of experimental data. *Arch. Toxicol.* 78, 252–268.
785 <https://doi.org/10.1007/s00204-003-0519-y>

786 Vaccher, V., Ingenbleek, L., Adegboye, A., Hossou, S.E., Koné, A.Z., Oyedele, A.D., Kisito, C.S.K.J.,
787 Dembélé, Y.K., Hu, R., Adbel Malak, I., Cariou, R., Vénisseau, A., Veyrand, B., Marchand, P.,
788 Eyangoh, S., Verger, P., Dervilly-Pinel, G., Leblanc, J.C., Le Bizec, B., 2020. Levels of
789 persistent organic pollutants (POPs) in foods from the first regional Sub-Saharan Africa Total
790 Diet Study. *Environ. Int.* 135, 105413. <https://doi.org/10.1016/j.envint.2019.105413>

791 Viant, M.R., Ebbels, T.M.D., Beger, R.D., Ekman, D.R., Epps, D.J.T., Kamp, H., Leonards, P.E.G.,
792 Loizou, G.D., MacRae, J.I., van Ravenzwaay, B., Rocca-Serra, P., Salek, R.M., Walk, T., Weber,
793 R.J.M., 2019. Use cases, best practice and reporting standards for metabolomics in regulatory
794 toxicology. *Nat. Commun.* 10. <https://doi.org/10.1038/s41467-019-10900-y>

795 Wahlang, B., Cameron Falkner, K., Clair, H.B., Al-Eryani, L., Prough, R.A., Christopher States, J.,
796 Coslo, D.M., Omiecinski, C.J., Cave, M.C., 2014. Human receptor activation by aroclor 1260, a
797 polychlorinated biphenyl mixture. *Toxicol. Sci.* 140, 283–297.
798 <https://doi.org/10.1093/toxsci/kfu083>

799 Wahlang, B., Hardesty, J.E., Jin, J., Falkner, K.C., Cave, M.C., 2019. Polychlorinated biphenyls and
800 nonalcoholic fatty liver disease. *Curr. Opin. Toxicol.* 14, 21–28.
801 <https://doi.org/10.1016/j.cotox.2019.06.001>

802 Walker, D.I., Marder, M.E., Yano, Y., Terrell, M., Liang, Y., Barr, D.B., Miller, G.W., Jones, D.P.,
803 Marcus, M., Pennell, K.D., 2019. Multigenerational metabolic profiling in the Michigan PBB
804 registry. *Environ. Res.* 172, 182–193. <https://doi.org/10.1016/j.envres.2019.02.018>

805 Wang, Q., Liu, D., Song, P., Zou, M.H., 2015. Tryptophan-kynurenine pathway is dysregulated in
806 inflammation, and immune activation. *Front. Biosci. - Landmark* 20, 1116–1143.
807 <https://doi.org/10.2741/4363>

808 Wang, X., Xu, Y., Song, X., Jia, Q., Zhang, X., Qian, Y., Qiu, J., 2019. Analysis of
809 glycerophospholipid metabolism after exposure to PCB153 in PC12 cells through targeted
810 lipidomics by UHPLC-MS/MS. *Ecotoxicol. Environ. Saf.* 169, 120–127.
811 <https://doi.org/10.1016/j.ecoenv.2018.11.006>

812 Weitekamp, C.A., Phillips, L.J., Carlson, L.M., DeLuca, N.M., Cohen Hubal, E.A., Lehmann, G.M.,
813 2021. A state-of-the-science review of polychlorinated biphenyl exposures at background levels:
814 Relative contributions of exposure routes. *Sci. Total Environ.* 776, 145912.
815 <https://doi.org/10.1016/j.scitotenv.2021.145912>

816 White, S.S., Birnbaum, L.S., 2009. An overview of the effects of dioxins and dioxin-like compounds
817 on vertebrates, as documented in human and ecological epidemiology. *J. Environ. Sci. Heal. -*
818 *Part C Environ. Carcinog. Ecotoxicol. Rev.* 27, 197–211.
819 <https://doi.org/10.1080/10590500903310047>

820 Wishart, D.S., 2016. Emerging applications of metabolomics in drug discovery and precision
821 medicine. *Nat. Rev. Drug Discov.* 15, 473–484. <https://doi.org/10.1038/nrd.2016.32>

822 Wishart, D.S., Feunang, Y.D., Marcu, A., Guo, A.C., Liang, K., Vázquez-Fresno, R., Sajed, T.,
823 Johnson, D., Li, C., Karu, N., Sayeeda, Z., Lo, E., Assempour, N., Berjanskii, M., Singhal, S.,
824 Arndt, D., Liang, Y., Badran, H., Grant, J., Serra-Cayuela, A., Liu, Y., Mandal, R., Neveu, V.,
825 Pon, A., Knox, C., Wilson, M., Manach, C., Scalbert, A., 2018. HMDB 4.0: The human
826 metabolome database for 2018. *Nucleic Acids Res.* 46, D608–D617.
827 <https://doi.org/10.1093/nar/gkx1089>

828 Xu, W., Wang, X., Cai, Z., 2013. Analytical chemistry of the persistent organic pollutants identified in
829 the Stockholm Convention: A review. *Anal. Chim. Acta* 790, 1–13.
830 <https://doi.org/10.1016/j.aca.2013.04.026>

831 Yang, C., Song, G., Lim, W., 2020. Effects of endocrine disrupting chemicals in pigs. *Environ. Pollut.*
832 263, 114505. <https://doi.org/10.1016/j.envpol.2020.114505>

833 Zhang, C.-Y., Flor, S., Ruiz, P., Ludewig, G., Lehmler, H.-J., 2021. Characterization of the Metabolic
834 Pathways of 4-Chlorobiphenyl (PCB3) in HepG2 Cells Using the Metabolite Profiles of Its

835 Hydroxylated Metabolites. *Environ. Sci. Technol.* <https://doi.org/10.1021/acs.est.1c01076>
836 Zhang, C.Y., Flor, S., Ruiz, P., Dhakal, R., Hu, X., Teesch, L.M., Ludewig, G., Lehmler, H.J., 2020.
837 3,3'-Dichlorobiphenyl Is Metabolized to a Complex Mixture of Oxidative Metabolites, including
838 Novel Methoxylated Metabolites, by HepG2 Cells. *Environ. Sci. Technol.* 54, 12345–12357.
839 <https://doi.org/10.1021/acs.est.0c03476>
840 Zhang, J., Yan, L., Tian, M., Huang, Q., Peng, S., Dong, S., Shen, H., 2012. The metabonomics of
841 combined dietary exposure to phthalates and polychlorinated biphenyls in mice. *J. Pharm.*
842 *Biomed. Anal.* 66, 287–297. <https://doi.org/10.1016/j.jpba.2012.03.045>

Figure captions

Figure 1. Stages of animal experimentation in this study, indicating the sampling days.

Figure 2. Score plots for PCA models built with the ‘metabolomics ESI-’ dataset before (a) and after (b, c) T0-centering. Number of principal components of each model: 7 (a) and 8 (b, c). The first and second principal components are represented in the score plots (a) and (b), while the first and fourth principal components are represented in the score plot (c). Group classes: *red circles* refer to samples from the acclimatization period, *green circles* indicate control samples from the exposure and the detoxification stages, and *blue circles* represent samples from exposed pigs collected in the periods of exposure and detoxification. Samples from the groups of control and exposed animals are indicated by (A,B) and (C-F), respectively.

Figure 3. Clustering heatmap and hierarchical analysis resulted from the NDL-PCB-related lipidomics study of serum samples analyzed by LC-HRMS under ESI+ conditions. In red / blue, the group of lipids with an increase / decrease in their concentration in serum associated with exposure to Aroclor 1260.

Figure 4. Evaluation of the PLS-DA model for the ‘lipidomics ESI-’ dataset: (a) PLS-DA score plot, (b) permutation tests for ‘control’ and ‘exposed’ groups. Group classes: *red circles* refer to samples from the acclimatization period, *green circles* indicate control samples from the exposure and the detoxification stages, and *blue circles* represent samples from exposed pigs collected in the periods of exposure and detoxification. Samples from the groups of control and exposed animal are indicated by (A,B) and (C-F), respectively.

Figure 5. Significantly disturbed metabolic pathways identified from pathway analysis by using the web service of MetaboAnalyst 4.0.

Table 1. Analysis of Variance (ANOVA)-Simultaneous Component Analysis (ASCA) of each of the datasets generated in this work. The confidence level was established at 95%.

Factor	Subject	Time	Exposure	Subject × Time	Subject × Exposure	Time × Exposure	Subject × Time × Exposure
<i>Dataset</i>	<i>p-value</i>						
Metabolomics (ESI+)	< 0.05	0.08	1.00	0.99	< 0.05	0.33	0.91
Metabolomics (ESI-)	< 0.05	0.30	1.00	0.94	< 0.05	0.38	0.82
Lipidomics (ESI+)	< 0.05	0.10	1.00	1.00	< 0.05	0.41	0.97
Lipidomics (ESI-)	< 0.05	< 0.05	1.00	1.00	< 0.05	0.52	0.98

Table 2. PLS-DA statistics of the models differentiating serum samples from pigs exposed (or not) to Aroclor 1260, as well as serum samples from the acclimatization period.

<i>Dataset</i>	Number of components	CV-ANOVA (<i>p</i>-value)	R2X (cum)	R2Y (cum)	Q2 (cum)	Classification accuracy
Metabolomics ESI+	3	1.025×10^{-16}	0.176	0.836	0.639	100 %
Metabolomics ESI-	2	1.436×10^{-19}	0.101	0.746	0.462	98.3 %
Lipidomics ESI+	2	1.534×10^{-17}	0.145	0.649	0.405	91.7 %
Lipidomics ESI-	2	2.597×10^{-19}	0.129	0.690	0.506	100 %

Table 3. Metabolites annotated (with confidence level 1 or 2) as possible biomarkers of exposure to Aroclor 1260 and previously found as relevant features in metabolomics datasets. Notes: ^a measured m/z of protonated ions; ^b m/z related to $[M+H-NH_3]^+$ ion; ^c m/z related to $[M-H-H_2O]^-$ ion. In red/blue, the group of metabolites with an increase/decrease in their concentration in serum associated with exposure to Aroclor 1260.

m/z^a	RT (min)	Ionization mode	Putative annotation	Confidence level of annotation	Variation of metabolite concentration levels in serum as a consequence of Aroclor 1260 exposure
114.0661	0.67	ESI+	creatinine	Level 1	
218.1385	1.1	ESI+	propionyl-L-carnitine	Level 1	
190.1185	0.67	ESI+	L-homocitrulline	Level 2	
214.2164	11.81	ESI+	tridecanamide	Level 2	
225.0519	1.56	ESI-	3-nitro-L-tyrosine	Level 1	
303.2331	13.24	ESI-	arachidonic acid	Level 1	
87.0087 ^c	0.77	ESI-	glyceric acid	Level 2	
89.0244	0.82	ESI-	glyceraldehyde	Level 2	
156.0667	6.97	ESI-	N-tiglylglycine	Level 2	
188.0705 ^b	2.38	ESI+	L-tryptophan	Level 1	
141.0051	0.56	ESI+	phosphono carbamimidate	Level 2	
231.1450	0.67	ESI+	L-alaninamide, L-alanyl-L-alanyl-	Level 2	
338.0867	4.56	ESI+	3-indoleformate glucuronide	Level 2	
230.1749	7.26	ESI+	N-decanoylglycine	Level 2	
432.3107	8.08	ESI+	3-hydroxy-5-cholenoylglycine	Level 2	
357.2785	9.04	ESI+	chola-4,6-dien-24-oic acid	Level 2	
467.3164	15.77	ESI+	L-eicosanoyl-glycero-3-phosphate	Level 2	
207.0775	1.42	ESI-	kynurenine	Level 1	
197.0432	1.28	ESI-	vanillylmandelic acid	Level 1	
201.1133	5.39	ESI-	sebacic acid	Level 1	
171.1391	9.91	ESI-	capric acid	Level 1	
129.0194 ^c	0.79	ESI-	2-hydroxyglutaric acid	Level 2	
145.0143	0.86	ESI-	2-oxoglutaric acid	Level 2	
130.0874	0.96	ESI-	DL-leucine	Level 2	
292.1403	0.96	ESI-	N-isopropyl-2'-deoxyadenosine	Level 2	
117.0558	2.29	ESI-	3-hydroxy-2-methyl-butanoic acid	Level 2	
188.0929	5.97	ESI-	N-lactyl-valine	Level 2	
172.0405	6.38	ESI-	quinaldic acid	Level 2	
211.0977	7.25	ESI-	3,4-methyleneazelaic acid	Level 2	
228.1605	7.27	ESI-	N-decanoylglycine	Level 2	
242.1763	7.86	ESI-	11-acetamidoundecanoic acid	Level 2	
243.1602	8.75	ESI-	brassylic acid	Level 2	
191.1079	9.2	ESI-	6-phenylcaproic acid	Level 2	

Figure 1

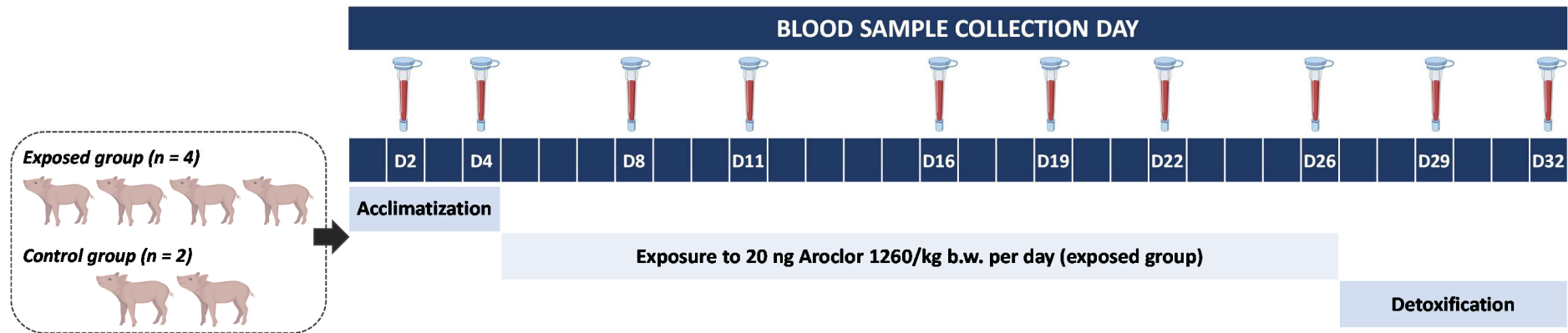


Figure 2

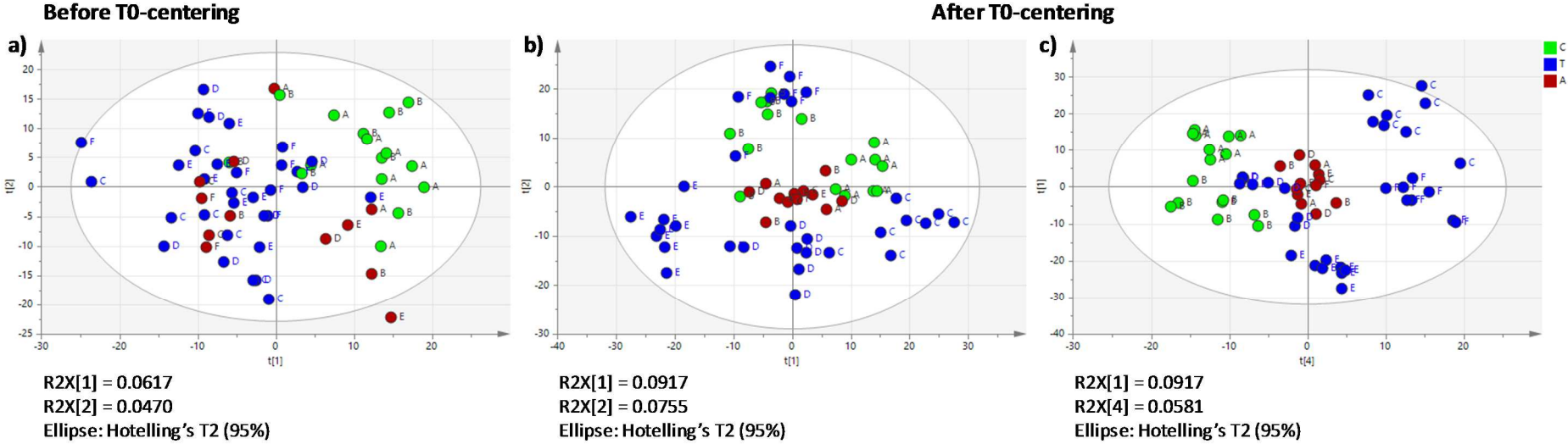


Figure 3

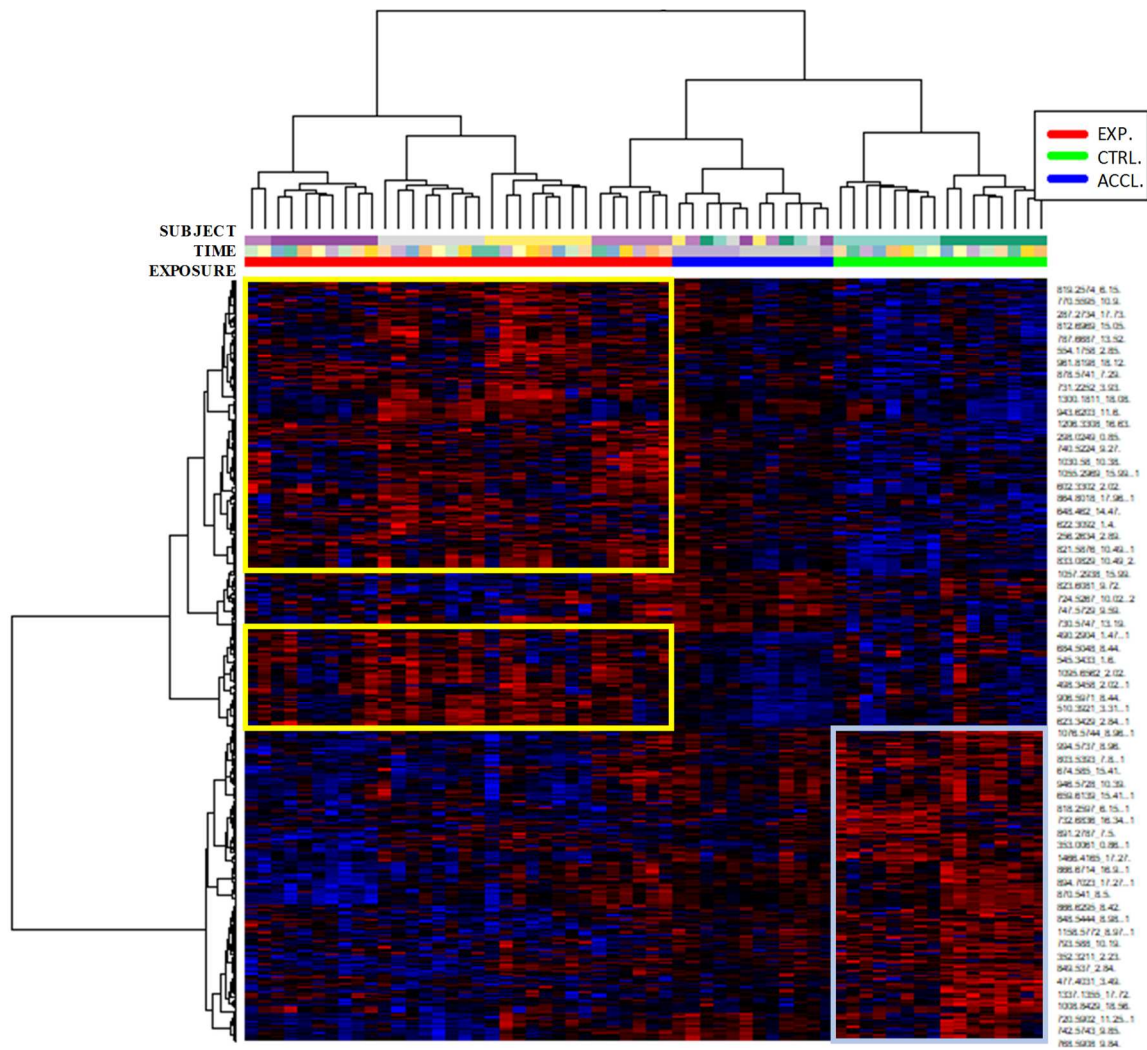


Figure 4

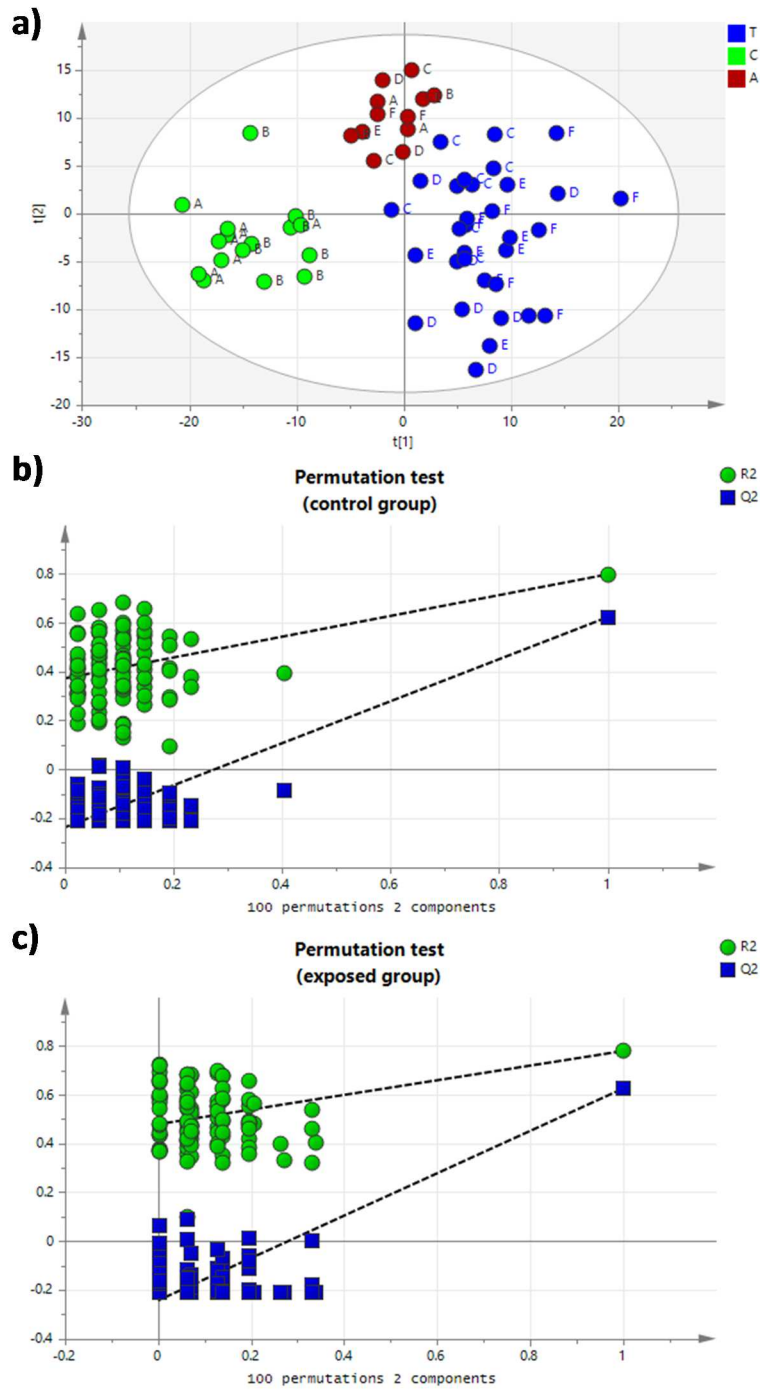
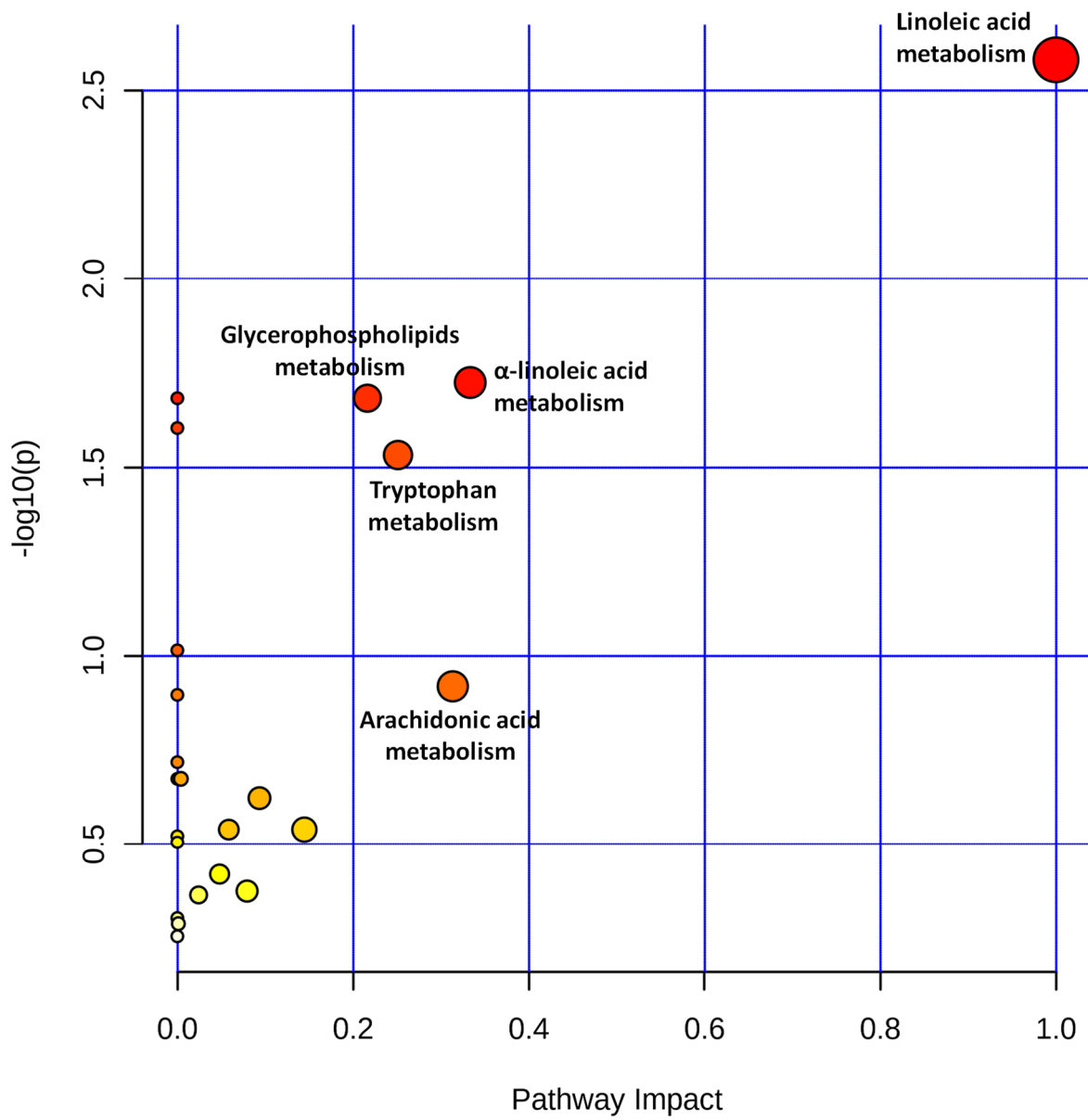
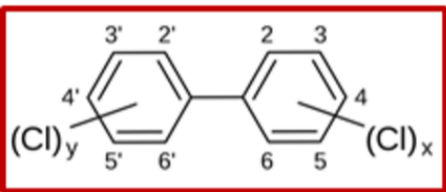
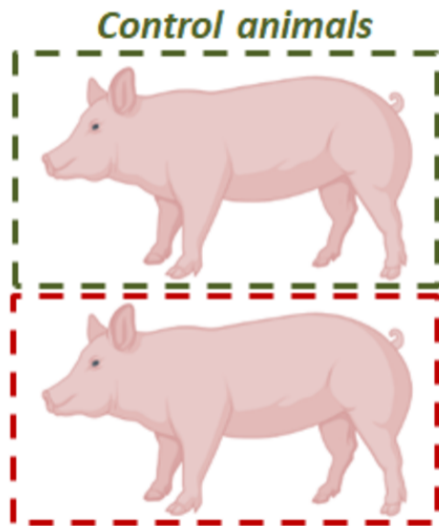


Figure 5





Low levels of exposure



Metabolomics and lipidomics study

